CBPF-NF-047/01

Ferromagnetic Resonance Studies of Cobalt Copper Alloys*

B.R. Pujada, E.H.C.P. Sinnecker, A.M. Rossi and *A.P. Guimarães*

Centro Brasileiro de Pesquisas Físicas
Rua Dr. Xavier Sigaud 150,
Rio de Janeiro - 22290-180, Brazil

Abstract

A systematic study of the ferromagnetic resonance (FMR) of the metastable Co_xCu_{100-x} granular alloy ribbons prepared by melt-spinning was made as a function of magnetic field angle relative to the normal to the plane of the ribbon, and annealing temperature. This study allowed changes in the Co grains to be followed. The measurements were performed at room temperature, for cobalt concentrations of x=3, 5, 10, and 15, with samples both as-cast and annealed for 1 hour at temperatures between 400 °C and 800 °C. In order to obtain the resonance fields and linewidths, the FMR spectra were fitted as a sum of absorption and dispersion functions. We observed that the resonance fields and linewidths vary in a systematic way with the angle of the magnetic field, with Co concentration, and with the annealing temperature. These results were interpreted using the Kittel equation for ferromagnetism, as well as simulations of the resonance field with the angle derived for spherical superparamagnetic grains. The analysis of the FMR spectra indicates grains whose mean diameters vary between 1.4 ± 0.1 nm and 4.1 ± 0.1 nm, depending on the cobalt concentration and annealing temperature. In addition, measurements of Co_5Cu_{95} annealed samples show a reduction in their magnetization at certain temperatures. This reduction is probably induced by a change in the crystal structure of the cobalt grains, or by the dissolution of the smaller ferromagnetic grains in the Cu matrix.

PACS: 75.50 Tt; 76.50 +g; 75.75 +a

*To be published in Physical Review B.

I INTRODUCTION

Granular magnetic materials are usually composed of magnetic grains with a few nanometers in size, dispersed in a non-magnetic metallic or insulating matrix [1]. Some examples can be found in the CoCu, FeCu, CoAg, FeAg and FeAu alloy systems. In every case, they are formed from two immiscible elements that have the tendency of segregating small magnetic particles into a non-magnetic matrix.

In the last years considerable theoretical and experimental effort was focused in the study of magnetic granular materials, specially since the discovery of the giant magnetoresistance (GMR) effect in these systems [2, 3]. This phenomenon is related with the appearance of an additional resistance due to electron scattering from nonaligned ferromagnetic grains. The GMR effect was first reported in magnetic multilayers [4], a finding which opened the possibility of a wide range of applications, notably in magnetic sensors and reading heads [5, 6]. The main advantage of using granular materials comes from the easy process of fabrication and the facility to tune their magnetic properties simply by changing their internal microstructure through a suitable thermal treatment.

Granular materials also present very interesting magnetic properties. The particles or grains, depending on size and temperature, may show either a superparamagnetic or a ferromagnetic character. Several experimental studies in these systems have shown that their magnetic properties are related to the shape of the sample, shape, size and concentration of the grains, fabrication process, and annealing temperature [7, 8, 9, 10, 11, 12, 13, 14, 15, 16].

Some ferromagnetic resonance (FMR) studies in magnetic granular alloys and films have shown that the shape, resonance field and linewidth of the FMR spectrum are sensitive to size, shape and concentration of the magnetic grains, to measuring temperature and heat treatment, and to the angle of the applied field with respect to the normal to the film plane [17, 18, 19, 20]. In the $Co_{22}Ag_{78}$ granular film Sang et al. [14] attributed the increase in the difference between the ferromagnetic resonance fields perpendicular and parallel to the film plane to changes in the grain shape in the process of thermal treatment, from roughly spherical to pancake shape. Pogorelov et al. [16] in their studies of heterogeneous Co_xAg_{1-x} films, observed differences in the FMR and magnetic behavior below and above the magnetic percolation concentration, of about 33 % in this case. For

very dilute samples, the model developed for spherical isotropic weakly interacting particles describes well the dependence of the resonance field with the angle of the applied field. For higher Co concentrations, above the magnetic percolation concentration, two split modes are observed, attributed to the coupling between magnetic moments of the grains, and the formation of ferromagnetic clusters.

Schmool et al. [19] observed in the X-band FMR study at room temperature of the $Co_{10}Cu_{90}$ granular alloy that the segregation of magnetic particles of cobalt in the FCC phase produces a decrease in the value of the resonance field. For high annealing temperatures, a change in the structure of the cobalt grains from FCC to HCP probably occurs. Recently, Lachowicz et al. [20] in an X-band FMR study as a function of temperature of $Co_{10}Cu_{90}$ granular alloys annealed at 773 K, interpreted their results assuming a distortion of the Co grains. The deformation of the cobalt particles, from spherical shape in the bulk material, into a spheroidal shape elongated in the direction of the ribbon length, was attributed to the compressive stress generated from the fact that the measurement was performed at a temperature lower than that of annealing.

In this work we present and analyze the ferromagnetic resonance spectra obtained at room temperature, for Co_xCu_{100-x} ribbons, measured as a function of angle, concentration, and thermal treatment.

II EXPERIMENTAL

Starting from a master alloy (Co_xCu_{100-x} with x=3, 5, 10 and 15) prepared by induction melting appropriate amounts of the pure elements in a He atmosphere, ribbons 70 μm thick were obtained by melt-spinning on a CuZr drum.

As-cast and annealed samples were investigated. Annealing was carried out in a conventional tubular furnace at several temperatures T_A (400 °C, 450 °C, 500 °C, 550 °C, 600 °C, 700 °C and 800 °C) in argon atmosphere for 1 hour in order to induce the precipitation of magnetic cobalt grains. For practical purposes the 'annealing temperature' of the as-cast ribbon was taken as 30 °C.

The room temperature FMR spectra of as-cast and annealed Co_xCu_{100-x} alloy samples for x=3, 5, 10 and 15 were obtained with a Bruker ESP300E spectrometer equipped with a ER 4102ST rectangular cavity, and operating at 9.6 GHz (X-band), with fixed microwave

power level of 1.0 mW and modulation amplitude of 1 G. In order to vary the angle θ of the magnetic field with the normal to the film plane, the sample was mounted on the tip of an external goniometer, introduced through a hole at the end of the cavity. Since the thickness of the ribbons is about 70 μm and the skin depth for the microwave is of only a few microns in the X band, the FMR signal comes mostly from regions near the surface of the samples.

The FMR spectra were least-squares fitted to obtain the linewidths and line positions (resonant fields H_r), after normalizing the spectra to the same absorption area. To account for the asymmetrical line shapes, the fitting function was a sum of a dispersion and an absorption function [21]. This procedure was found to be advantageous in order that changes in line shape did not mask the variation of H_r, or linewidth, with the experimental parameters.

In addition, room temperature magnetization measurements for Co_5Cu_{95} annealed at different temperatures were made with a superconducting quantum interference device (SQUID) magnetometer. The measurements were performed parallel and perpendicular to the plane of the ribbons with a field of 4 T.

Fig.1 presents in schematic form the geometry used in the study of the granular alloy ribbons. $\vec{H}$ represents the applied magnetic field and $\vec{M}$ the magnetization of the grain.

III FMR IN GRANULAR ALLOYS

The magnetization of a granular magnetic system composed of small superparamagnetic grains in the presence of a magnetic field can be described by

$$M = M_s \int L(\frac{\mu H}{k_B T}) f(v) dv \tag{1}$$

where M_s is the saturation magnetization of the grain, μ is the magnetic moment of the grain of volume v, $f(v)$ the distribution function of the grain volume, k_B the Boltzmann constant and $L(\mu H/k_B T)$ the Langevin function defined by

$$L(\frac{\mu H}{k_B T}) = \coth(\frac{\mu H}{k_B T}) - \frac{k_B T}{\mu H} \tag{2}$$

In the case of spherical grains with uniform volume v, the magnetization can be represented by

$$M = M_s\{\coth(\frac{\mu H}{k_B T}) - \frac{k_B T}{\mu H}\} \tag{3}$$

where $\mu = vM_s$.

The magnetic free energy density for granular alloys with a volume fraction f and magnetization of the grain $\vec{M}$ can be approximated by [22]:

$$F = -f\vec{H}.\vec{M} + \frac{1}{2}f\vec{M}.[f\widehat{N} + (1-f)\widehat{N_g}].\vec{M} \tag{4}$$

where $\widehat{N}$ and $\widehat{N_g}$ represent the demagnetizing tensors of the sample and grain, respectively.

In the simplified picture of Fig. 1 the grain has spherical shape and the sample has the shape of a thin plate; in this situation the demagnetizing tensors can be represented by

$$\widehat{N} = (0, 0, 4\pi), \qquad \widehat{N_g} = \frac{4\pi}{3}(1, 1, 1) \tag{5}$$

Then, making use of Fig. 1, Eq. (4) and Eq. (5), the free energy density can be written in the following form

$$F = -fHM\sin\alpha\cos(\varphi - \theta) + 2\pi M^2 f^2 \sin^2\alpha\cos^2\varphi + \frac{2\pi}{3}M^2 f(1-f) \tag{6}$$

The equilibrium orientation of the magnetization $\vec{M}$ is defined by the angles α_{eq} and φ_{eq} such that the free energy density is a minimum

$$\begin{aligned} \alpha_{eq} &= \frac{\pi}{2} \\ H\sin(\varphi_{eq} - \theta) &= 4\pi M f \sin\varphi_{eq}\cos\varphi_{eq} \end{aligned} \tag{7}$$

In the non-equilibrium case, which arises when the magnetization is perturbed from the equilibrium position, the frequency of resonance or equivalently the resonance field can be derived from the equation [23]:

$$(\frac{\omega}{\gamma})^2 = H_0^2 = \frac{1}{M^2 f^2 \sin^2\alpha}\{F_{\alpha\alpha}F_{\varphi\varphi} - F_{\alpha\varphi}^2\}_{(\alpha_{eq},\varphi_{eq})} \tag{8}$$

where $F_{\alpha\alpha}$ represents the second derivatives with respect to α of the free energy density.

Now, considering Eq. (6) and Eq. (7) together with the fact that the magnetization is undersaturated, and making the calculations of Eq. (8), it follows

$$H_r(\theta) = H_o\{1 + \frac{2\pi f M}{H_o}(3\cos^2\theta - 1)\} \tag{9}$$

where H_o can be obtained from the Kittel equations for ferromagnetism [24]

$$\begin{aligned} {H_o}^2 &= H_{\|}(H_{\|} + 4\pi M_{eff}) \\ H_o &= H_{\perp} - 4\pi M_{eff} \end{aligned} \tag{10}$$

where $H_{\|}$ and $H_{\perp}$ are the resonance fields for $\theta = 90^o$ and $\theta = 0^o$, respectively, and M_{eff} is the effective magnetization. Then, replacing the magnetization obtained in Eq. (3), it finally follows

$$H_r(\theta) = H_o\{1 + \frac{2\pi f M_s}{H_o}[\coth(\frac{\mu H}{k_B T}) - \frac{k_B T}{\mu H}](3\cos^2\theta - 1)\} \tag{11}$$

where $\mu = vM_s$. From this equation the volume and therefore the diameter of the grain v can be calculated.

IV EXPERIMENTAL RESULTS

The FMR spectra were obtained for the Co_xCu_{100-x} samples, annealed and as-cast; in the case of x=3 the signals of the as-cast samples are very weak, and therefore a proper spectrum could not be studied. Fig. 2 (a) displays a sequence of FMR spectra as a function of the angle θ for Co_5Cu_{95} annealed at 500 °C, illustrating the shift of the resonance line towards lower fields as the sample is rotated from $\theta = 0^o$, where H_r= 3523 Oe (perpendicular to the ribbon plane) to $\theta = 90^o$, where H_r=2951 Oe (parallel to the ribbon plane). A reduction of the linewidth from 958 Oe to 832 Oe, when the angle is changed from $\theta = 0^o$ to $\theta = 90^o$ is also observed. Fig. 2 (b) shows the experimental FMR spectrum and its computer fit obtained as a sum of absorption and dispersion functions for as-cast Co_5Cu_{95}; it is observed that the fit reproduces the experimental spectrum fairly well.

The behavior of H_r with the angle shows a maximum at θ=0° (Fig. 3), but at certain temperatures of annealing T_A, H_r shows a sharp maximum not exactly at 0 degress, and

therefore the model represented by Eq. (11) is not strictly applicable. The maximum annealing temperatures studied were those for which this deviation was observed, and this varies with the concentration, for example for x=3, T_A=700 °C, for x=5 and 10, T_A=800 °C, and for x=15, T_A=500 °C. A reduction of the FMR signal is also observed for samples annealed above certain temperatures (e.g., Co_5Cu_{95} annealed above 600°C).

Fig. 3 shows the angular dependence of the resonance field derived from the fit of the FMR spectra for the samples with x=3, 5, 10 and 15, as-cast and annealed at temperatures T_A. The lines (continuous and dotted) are computer simulations using the function of Eq. (11). A series of features can be observed: firstly, a good agreement between the experimental results and the theoretical curve of Eq. (11) for the as-cast ribbons for both the Co_5Cu_{95} and $Co_{10}Cu_{90}$ samples (Fig. 3 a-b). The same result is obtained for the $Co_{15}Cu_{85}$ sample in the as-cast form. Good simulations are obtained for all samples annealed at temperatures lower than 600 °C for x=3 and 5, and 500 °C for x=10 and 15. Fig. 3 (c) shows the case of Co_3Cu_{97} and $Co_{15}Cu_{85}$ samples annealed at 500 °C and 450 °C, respectively. Fig. 3 (b) shows, for $Co_{10}Cu_{90}$ annealed at 500 °C, that the model based on the assumption of spherical superparamagnetic grains with weak interactions does not provide a good simulation of the curve of resonance field versus angle θ.

Fig. 4 illustrates the variation of the resonance field H_r for each value of θ, as a function of T_A for the Co_xCu_{100-x} alloys with x=3, 5, 10 and 15. We can observe some features common to all the samples. In the first place the resonance field shows little difference from as-cast up to approximately 400 °C. For temperatures between 450 °C and 550 °C, H_r perpendicular ($\theta = 0°$) and parallel to the ribbon plane ($\theta = 90°$), for x=3, 5 and 10, move toward high and low fields, respectively. The resulting difference $H_r(0°) - H_r(90°)$ is small for Co_3Cu_{97}, and higher for the $Co_{10}Cu_{90}$ samples. For T_A above 550 °C H_r decreases in value for temperatures up to 600 °C for x=3, 700 °C for x=5, and 800 °C for x=10. For x=3, 5 and 10 one observes an increase in H_r at temperatures between 600 °C and 700 °C. The angular dependence of the resonance field for x=15 could not be simulated with the function of Eq. (11) for annealing temperatures equal or above 500 °C. Therefore the effect discussed above was not studied in this more concentrated sample. We think that these differences can be related to marked changes in the characteristics internal structure of the granular alloy.

From the curves of H_r versus θ shown in Fig. 3 for the as-cast samples of Co_5Cu_{95}

and $Co_{10}Cu_{90}$, the average grain diameters derived from Eq. (11) are 2.1 $\pm$0.1 nm and 1.7 $\pm$0.1 nm, respectively. Fig. 5 shows the evolution of the average diameter of the cobalt grain versus T_A, which was determined from the simulation of Eq. (11) (continuous line) and for the usual form, i.e., by determining the field at which the derivative of the signal crosses the baseline (doted lines), for the samples with x=3, 5, and 10. For the maximum temperatures of annealing T_A for the samples, the simulation of the resonance field H_r versus the angle θ from Eq. (11) was not performed because the shape of the curve of H_r versus the angle θ does not change in a systematic way as shown in Fig. 3, and therefore the diameter was not calculated. The behavior of these curves with T_A in Fig. 5 is the same for all the Co_xCu_{100-x} alloy samples. For the sake of simplicity M_s was assumed constant in the calculation of the resonance field H_r given by Eq. (11), and therefore in obtaining the diameter d. For the $Co_{15}Cu_{85}$ alloy samples annealed up to 450 °C the diameters obtained were of approximately 2.8 nm $\pm$0.1.

Fig. 6 shows the magnetization M of the Co_5Cu_{95} ribbon, as a function of annealing temperature, with the magnetic field applied parallel or perpendicular to the plane of the ribbon. An increase is noted in the values of M for temperatures up to 550 °C and 600 °C, for fields perpendicular and parallel, respectively. For temperatures of annealing above 550 °C and 600 °C a slight decrease in the perpendicular and parallel magnetization of saturation is observed. In addition, the difference between perpendicular and parallel magnetization is larger at approximately 500 °C.

The evolution of the FMR linewidth with annealing temperature is shown in Fig. 7 for Co_5Cu_{95} and $Co_{10}Cu_{90}$. For these samples we can see in the first place small variations in the linewidth from as-cast to annealed at 500 °C. For high T_A the linewidth for samples of both concentrations increases rapidly and the difference between linewidths perpendicular and parallel is larger.

V DISCUSSION AND CONCLUSIONS

In this study the FMR spectra were fitted as a sum of absorption and dispersion functions. We found that this fitting of experimental lines is good for temperatures of treatment up to approximately 500 °C. In addition, the ratio of absorption to dispersion terms in the spectra changes with the annealing. This ratio is related to the ratio A/B (where A and

B are, respectively, amplitudes of the positive and negatives lobes of the FMR spectrum). For temperatures T_A lower that 500 °C this ratio is independent of the angle θ, as one would in principle expect for nearly spherical cobalt grains. For higher temperatures of treatment this ratio increases, and becomes dependent on the angle θ. From these results one may conclude that this method of fitting the FMR spectra is valid for samples treated at temperatures up to 500 °C in which the average grain volume is small.

We have found that the behavior of the FMR field, H_r, as a function of the angle θ, can be well described with a model of spherical superparamagnetic grains for Co_xCu_{100-x} melt-spun ribbon from as-cast and annealed at temperatures below 500 °C. For Co_5Cu_{95} the range of applicability of the model is wider than that for the other samples.

For the case of samples with higher concentrations and higher annealing temperatures (e.g., x=10 and 15), a large discrepancy was observed between the experimental results and the simulations with Eq. (11). The differences could probably be attributed to changes in the shape of the grains with thermal treatment, therefore invalidating the application of the model. We attempted to account for small variations in the shape of the grains from spherical to spheroidal, by introducing a demagnetizing factor $\widehat{N_g} = 4\pi(1-2\epsilon, \epsilon, \epsilon)$ where $1/3 < \epsilon < 1/2$. Introducing these factors, a different dependence of the resonance field with θ and ϵ parameters was obtained, however, this change in the model does not improve the simulations of the curves for samples annealed at higher temperatures.

Other explanations for the disagreement between simulations of $H_r(\theta)$ and experimental results could be the formation of grain clusters, the interactions between grains, formation of multidomain grains or an increase in the anisotropy of the sample.

In Fig. 3 (b), for $Co_{10}Cu_{90}$ annealed at 500 °C, it is observed that the simulation only reproduces the experimental values for θ equal to 0° and 90°, although the overall agreement is bad. The conclusion we can draw is that the determination of grain shape and volume based on the FMR spectra measured with only two directions of the field, parallel and perpendicular to the ribbon plane as sometimes reported in the literature, may lead to errors.

The results of resonance field versus annealing temperature for Co_5Cu_{95}, $Co_{10}Cu_{90}$ and $Co_{15}Cu_{85}$ (Fig. 4) do not show important variations of the resonance field between the as-cast sample and the samples annealed at 450 °C. This can be understood from the

fact that although the thermal treatment initiates a phase segregation and allows the rearrangement of the magnetic grains, it gives rise to grains with similar average diameters and a nearly spherical shape.

For T_A between 400 ° and 550 °C, an increase in the difference between the resonance fields perpendicular and parallel to the ribbon plane is observed (Fig. 4). Sang et al. [14] attributed this behavior to an increase of the demagnetizing field of the grains perpendicular to the plane of the ribbon and a decrease in the direction parallel to the plane of the ribbon. This arises from a growth of the grain dimensions preferentially along directions parallel to the plane of the ribbon during the annealing process [25, 26]. According to this explanation, the grains in the $Co_{10}Cu_{90}$ sample must present a langer increase in their dimensions along the plane of the ribbon, and consequently the experimental data cannot be well simulated with the present model. This behavior can also be observed in the other samples, but its effect is not appreciable. The increase in the mean diameter of the magnetic grains for Co_3Cu_{97} and Co_5Cu_{95} samples in Fig. 4 suggests that the increase in the dimensions on the plane is more significant than the reduction in the perpendicular direction.

The observed changes of H_r perpendicular to the ribbon plane towards lower field, for the samples with x=3, 5, and 10 annealed at temperature higher than 550 °C are shown in Fig. 4. This can be explained if one considers an increase in the anisotropy field H_a perpendicular to the plane of the ribbon and therefore H_r perpendicular ($\theta = 0°$) could decrease with increasing annealing temperatures.

The average grain diameters obtained in this study are comparable to those of a cobalt particle with blocking temperature of 300 °K (d=5 nm). The average grain diameter for samples with x=3, 5 and 10 increases with annealing temperature for samples annealed from 400 °C to 600 °C, varying from 1.4 ± 0.1 nm to 4.1 ± 0.1 nm. Above 600 °C, the observed decrease in the diameter d in Co_5Cu_{95} can be correlated with the reduction of the magnetization as shown in Fig. 6. This may indicate that if this variation of M had been taken into account in the model, there would result in a different dependence of the grain volume with T_A. In the correlation of the FMR results with the magnetization data, it should be pointed out that the former measures the outer parts of the ribbons, whereas the latter samples the whole volume.

The initial increase of M observed in Fig. 6 can be attributed to the growth of the

Co grains, and consequently the increase in the proportion of those grains that show ferromagnetic behavior. The fact that the magnetization is larger for H perpendicular to the plane of the ribbon than for H parallel is possibly related to the increase of the anisotropy field in the perpendicular direction. The same effect was observed in granular CoAg films [8]. The observed decrease in the magnetization for samples treated above 550 °C may have two reasons. It may be related to the onset of the change in the crystal phase of cobalt, from FCC to HCP, detected with NMR [27], since it is known that HCP cobalt has a smaller magnetization. Or else, this decrease may be associated with the dissolution at higher temperatures of the smaller ferromagnetic grains in the matrix, as observed by other authors [28, 13].

In a metallic system such as the CoCu alloys one should expect two contributions to the FMR linewidth: one related to the inhomogeneity of the internal field, and another to the spread of the crystalline axis directions for the different Co grains [29]. The experimental results in Fig. 7 show small variations in the FMR linewidth from as-cast to 500 °C, the same behavior was observed for x=15 up to 400 °C, and for x=3 up to 500 °C. We think that although the particle size of the cobalt grain shows a substantial increase from as-cast to 500 °C (Fig. 5), this increase is homogeneous and therefore as shown by Rodbell [25], the FMR spectra will retain its linewidth. Above 500 °C a market increase in the linewidth is observed principally in the perpendicular direction. Although the formation of multidomain grains can cause an increase in the linewidth [12], this is not plausible in our system, since the grain diameters are much smaller that the critical size for the formation of multidomain particles. Lachowicz and co-workers [20] in FMR measurements at different temperatures explain the linewidth broadening as due to an increase in the anisotropy constant K_1, the linewidth being of the order of $|K_1|/M_s$.

For higher temperatures we also observed an increase in the grain volume, but the deformation of the grain shape is inhomogeneous, and as pointed out by Rodbell [25] this generates an increase in the linewidth. This behavior can be related to the appearance of a net increase in the anisotropy perpendicular to the plane of the ribbon. Therefore we conclude that the inhomogeneous deformation of the cobalt grains in the superparamagnetic regime and not the increase in their size, is probably responsable for the increase in the linewidth. This change in the anisotropy would also explain the dependence of H_r measured for T_A higher that 500 °C, as mentioned above.

ACKNOWLEDGMENTS

This work was supported by the Brazilian agencies FAPERJ and CNPq; the authors thank P. Tiberto, P. Allia and F. Vinai (IEN Galileo Ferraris, Torino, Italy) for kindly supplying the samples used in this study.

Figure Captions

Fig. 1 Schematic diagram showing the granular alloy ribbon containing spherical magnetic grains, the applied magnetic field **H**, and the magnetization of the grain **M**. The plane of the ribbon is parallel to the xy plane and M_{yz} represents the projection of **M** onto the yz plane.

Fig. 2 Typical X-band FMR spectra at room temperature: (a) variation of the FMR spectra of Co_5Cu_{95} alloy sample annealed at 500 °C with the angle θ; (b) FMR spectrum of the Co_5Cu_{95} as-cast alloy (triangles); the solid line represents the computer fit to a sum of absorption and dispersion functions.

Fig. 3 Angular dependence of the FMR resonance fields H_r for (a) Co_5Cu_{95} as-cast and annealed at 700 °C, (b) $Co_{10}Cu_{90}$ as-cast and annealed at 500 °C, and (c) Co_3Cu_{97} annealed at 500 °C and $Co_{15}Cu_{85}$ annealed at 450 °C. The values of H_r were obtained from the computer fits to the experimental room temperature X-band FMR spectra. The solid and doted lines are the computer simulations using Eq. (11).

Fig. 4 Room temperature FMR resonance field for each angle θ, as a function of annealing temperatures for (a) Co_3Cu_{97}, (b) Co_5Cu_{95}, (c) $Co_{10}Cu_{90}$ and (d) $Co_{15}Cu_{85}$ granular alloys.

Fig. 5 Average diameter d as a function of the annealing temperature for (a) Co_3Cu_{97}, (b) Co_5Cu_{95} and (c) $Co_{10}Cu_{90}$. The filled and open triangles represent the values of the diameter obtained from Eq. (11), both from fits of absorption and dispersion, and by the conventional method.

Fig. 6 Room temperature saturation magnetization versus annealing temperature for the bulk Co_5Cu_{95} samples, measured with a field of 4 T, either parallel or perpendicular to the plane of the ribbon.

Fig. 7 Room temperature FMR linewidth for each angle θ, as a function of annealing temperature for samples of the granular alloys Co_5Cu_{95} (a) and $Co_{10}Cu_{90}$ (b).

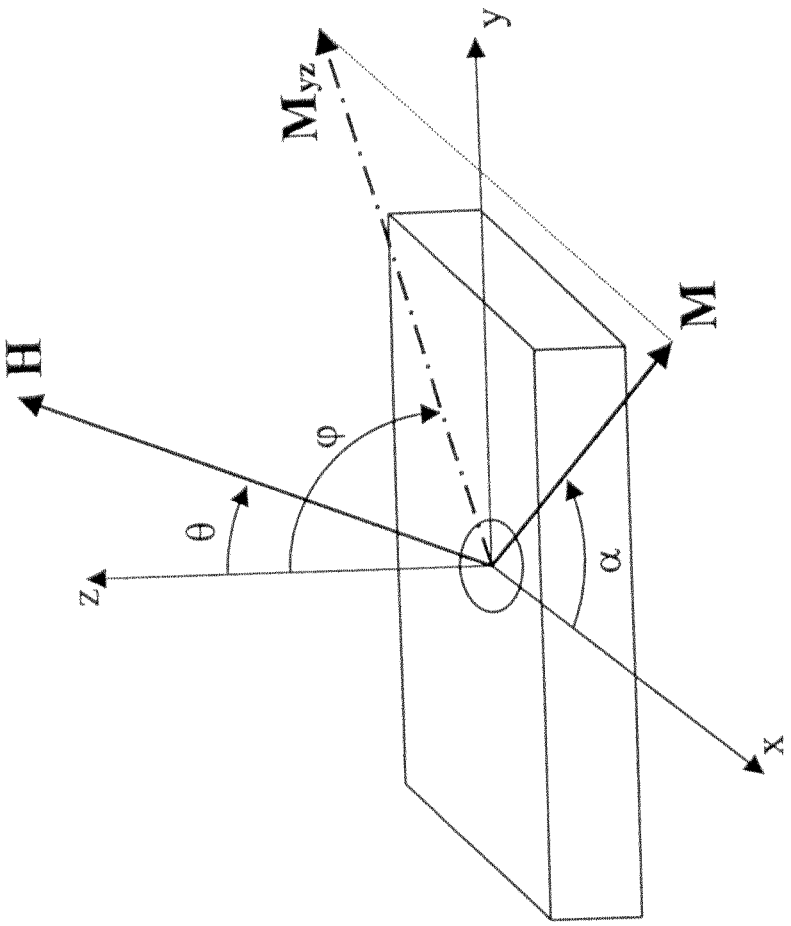
y
$\mathbf{M}_{yz}$
M
H
φ
θ
α
z
x

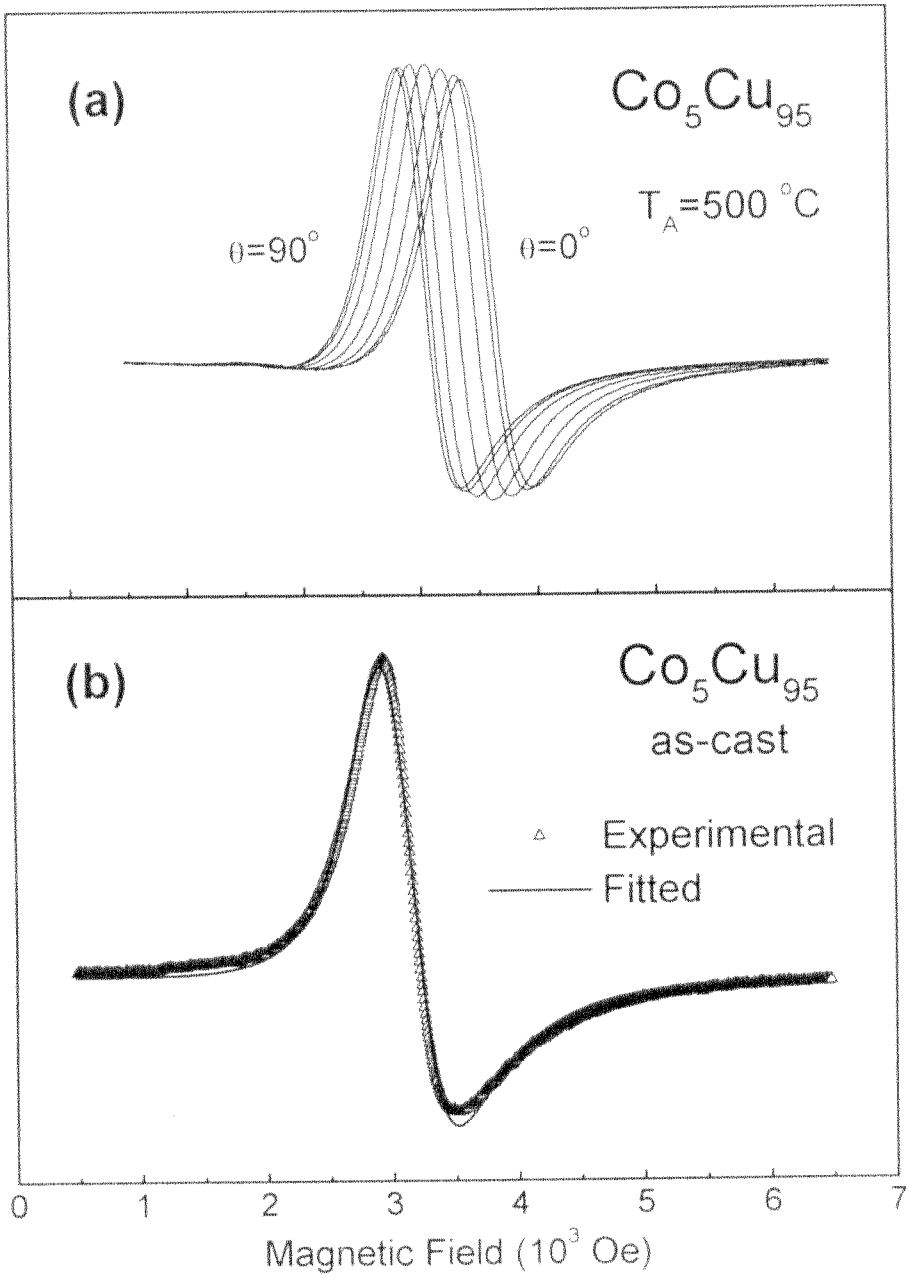
(a)
Co_5Cu_{95}
T_A=500 °C
θ=90°
θ=0°
(b)
Co_5Cu_{95}
as-cast
Experimental
Fitted
0
1
2
3
4
5
6
7
Magnetic Field (10^3 Oe)

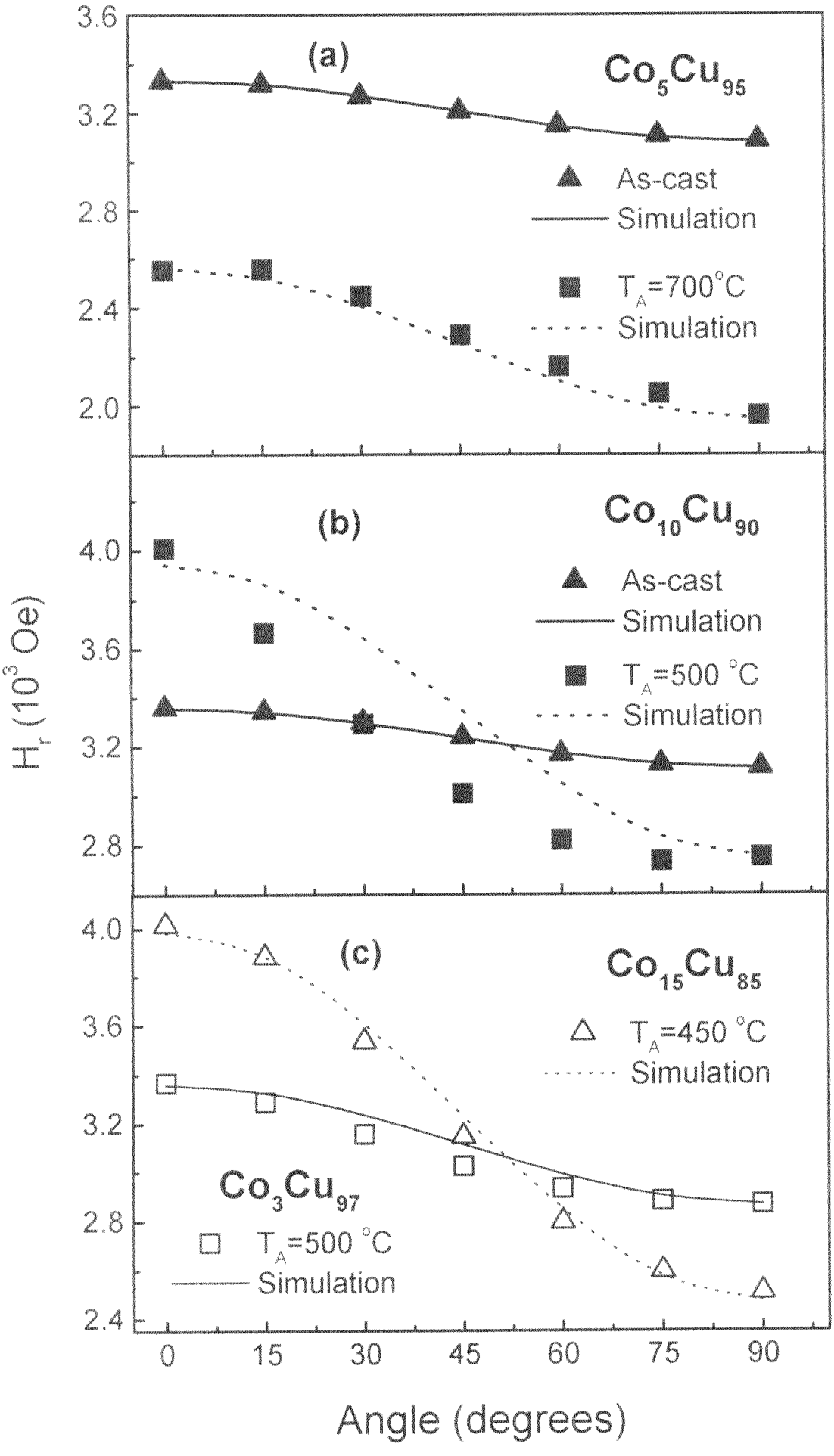
(a)
Co5Cu95
As-cast
Simulation
TA=700°C
Simulation
(b)
Co10Cu90
As-cast
Simulation
TA=500 °C
Simulation
(c)
Co15Cu85
TA=450 °C
Simulation
Co3Cu97
TA=500 °C
Simulation
Hr (10^3 Oe)
Angle (degrees)

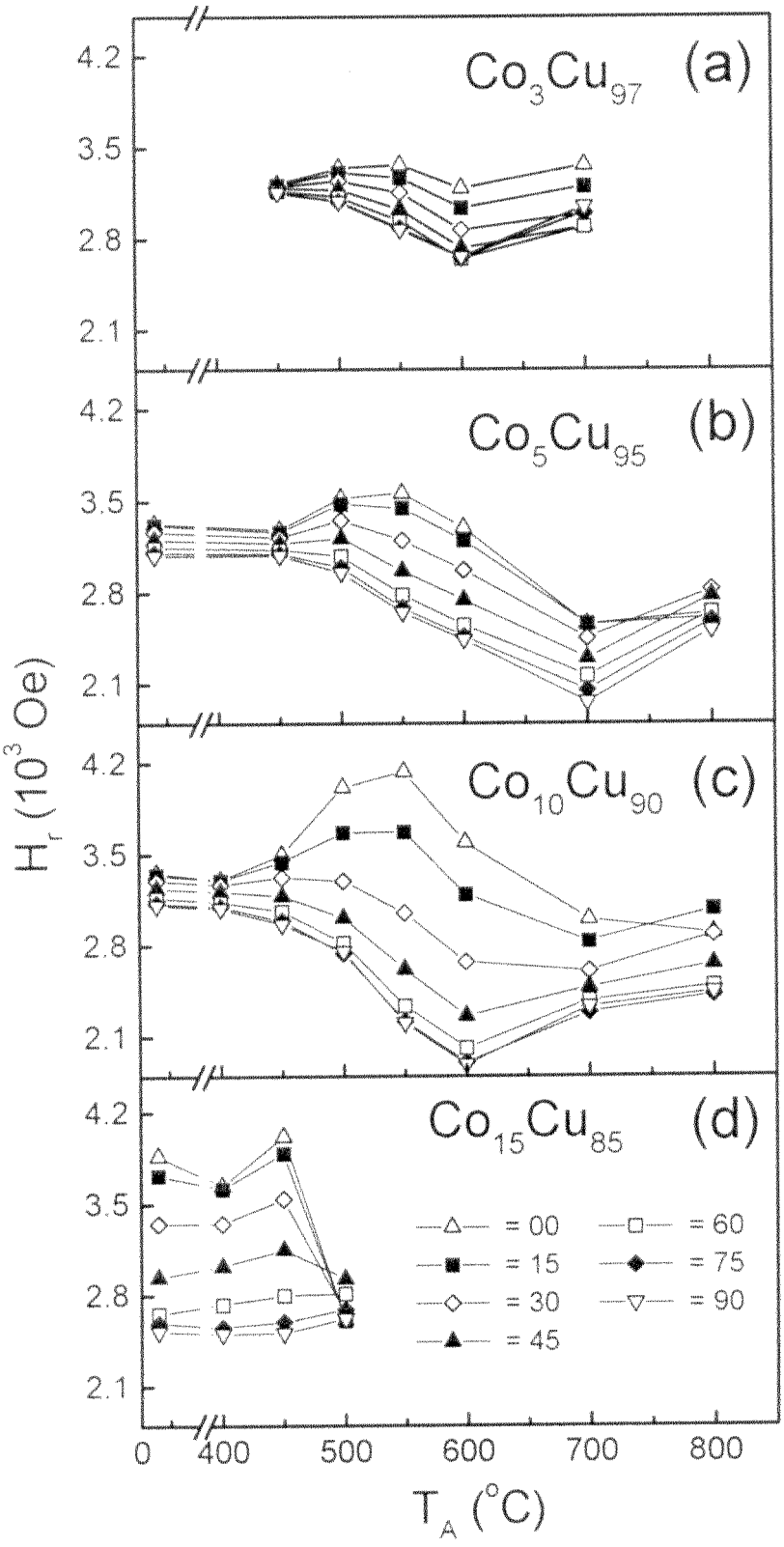
Co3Cu97 (a)
Co5Cu95 (b)
Co10Cu90 (c)
Co15Cu85 (d)
Hr (10^3 Oe)
TA (°C)
4.2
3.5
2.8
2.1
0
400
500
600
700
800
= 00
= 15
= 30
= 45
= 60
= 75
= 90

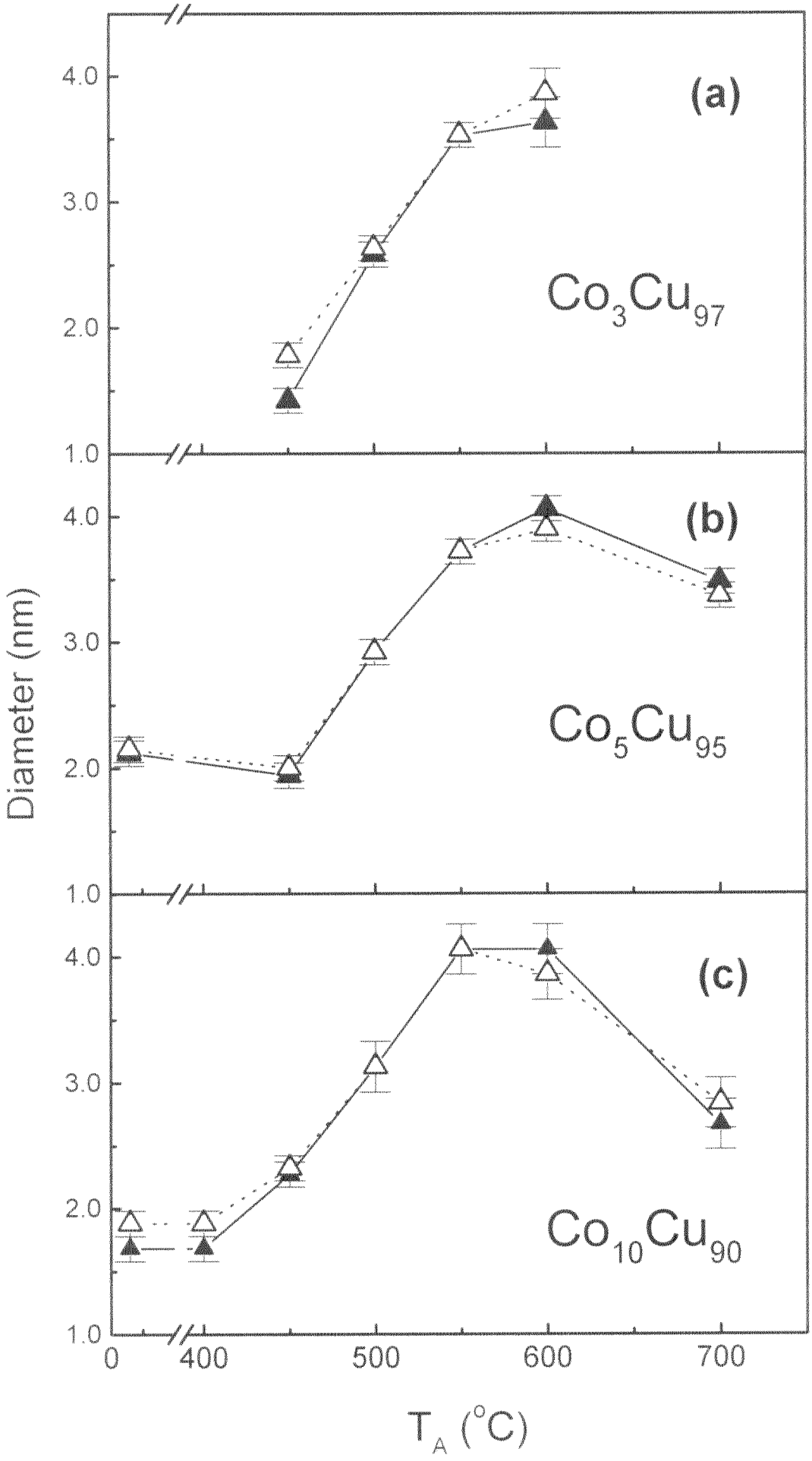
(a)
Co_3Cu_{97}
(b)
Co_5Cu_{95}
(c)
$Co_{10}Cu_{90}$
Diameter (nm)
T_A (°C)
1.0
2.0
3.0
4.0
0
400
500
600
700

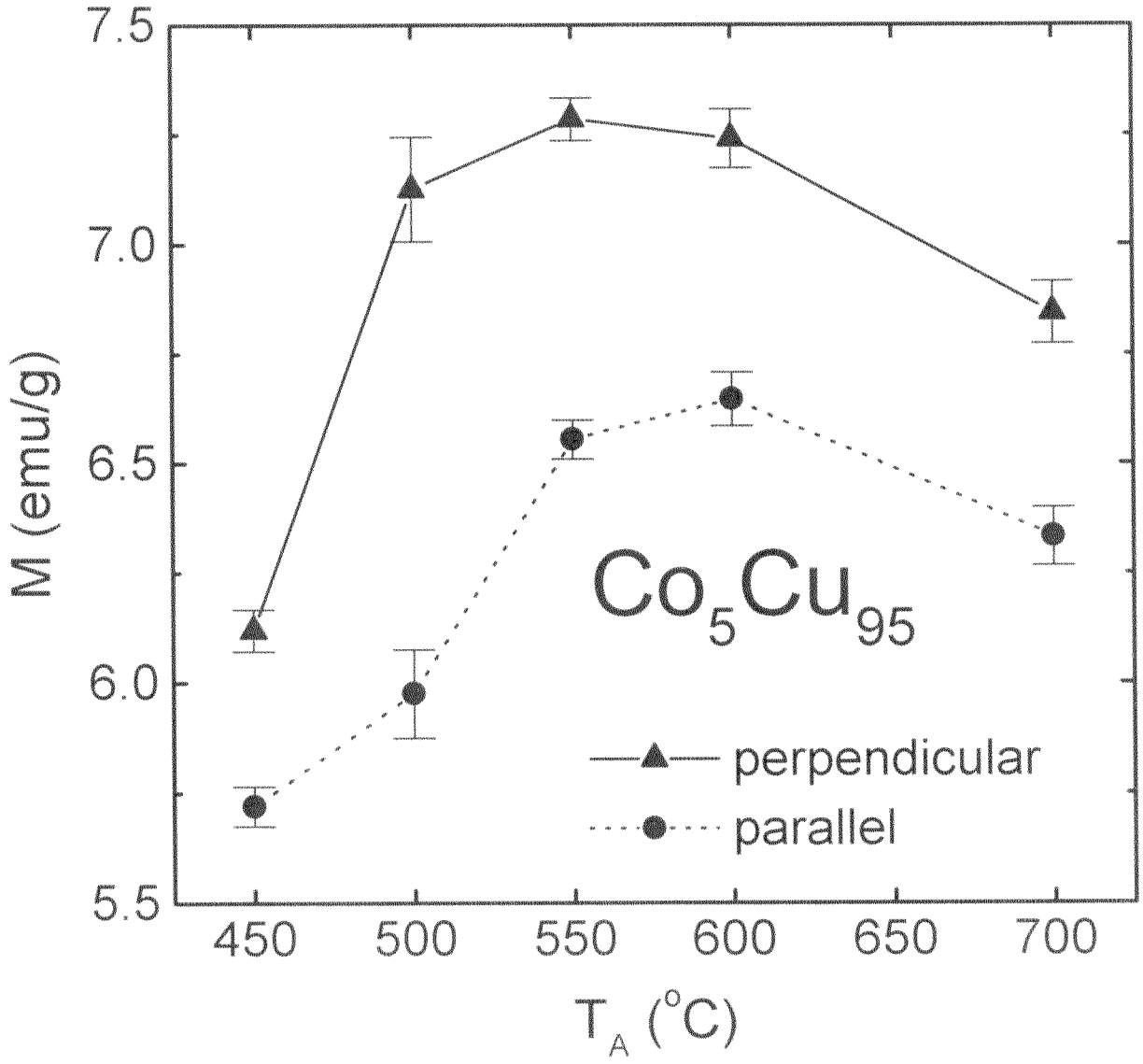
7.5
7.0
6.5
6.0
5.5
M (emu/g)
450
500
550
600
650
700
T_A (°C)
Co_5Cu_{95}
perpendicular
parallel

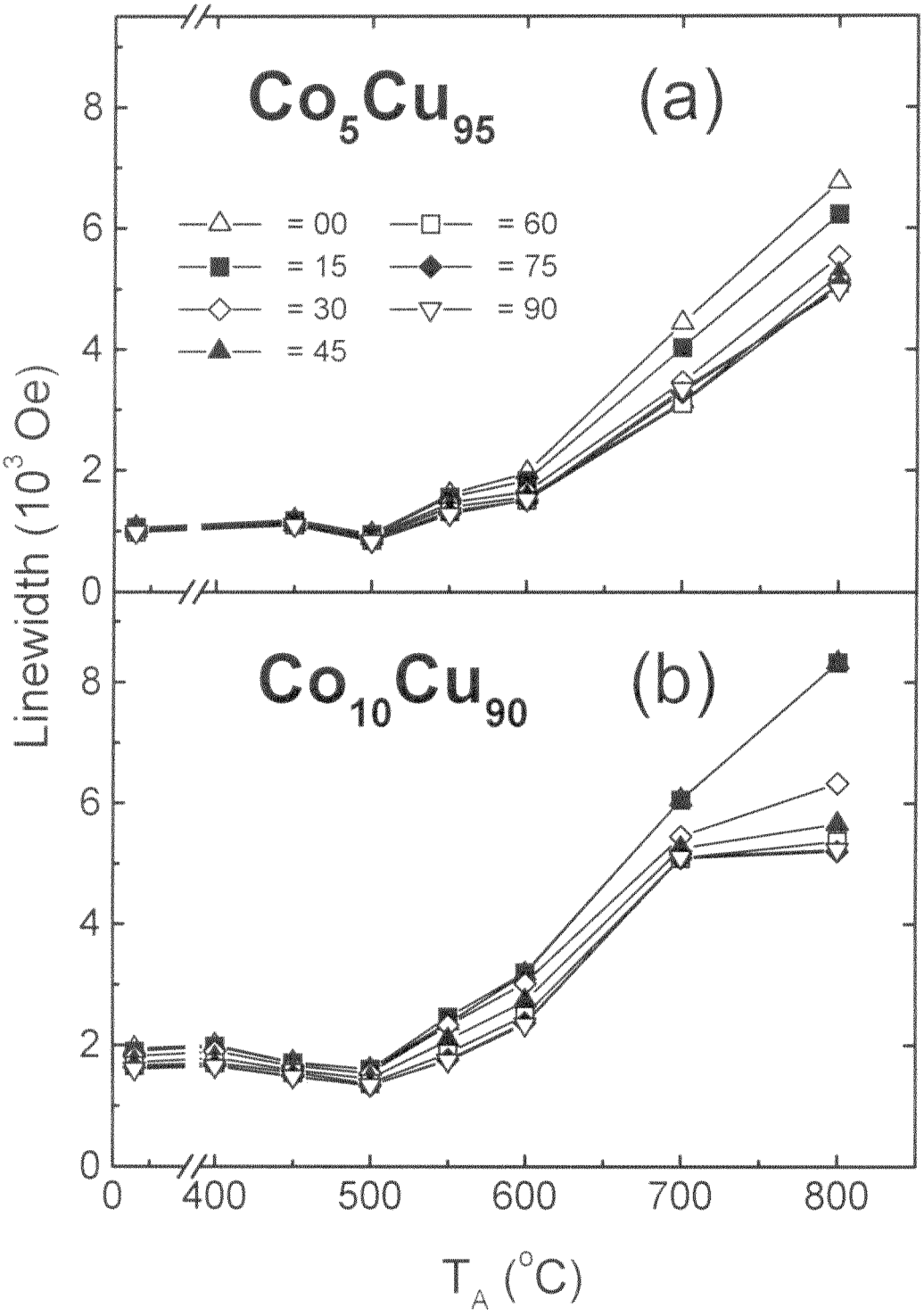
Co5Cu95
(a)
= 00
= 15
= 30
= 45
= 60
= 75
= 90
Co10Cu90
(b)
Linewidth (10^3 Oe)
T_A (°C)
0
2
4
6
8
400
500
600
700
800

References

[1] C.L. Chien, *Ann. Rev. Mater. Sci.*, **25**, 129 (1995).

[2] A.E. Berkowitz, J.R. Mitchell, M.J. Carey, A.P. Young, S. Zhang, F.E. Spada, F.T. Parker, A. Hutten and G. Thomas, *Phys. Rev. Lett.*, **68**, 3745 (1992).

[3] J.Q. Xiao, J.S. Jiang and C.L. Chien, *Phys. Rev. Lett.*, **68**, 3749 (1992).

[4] M.N. Baibich, J.M. Broto, A. Fert, F. Nguyen van Dau, F. Petroff, P. Etrenne, G. Creuzet, A. Friederich, and J. Chazelez, *Phys. Rev. Lett.*, **61**, 2472 (1988).

[5] R.L. White, *IEEE Trans. Magn.*, **28**, 2482 (1992).

[6] G.A. Prinz, *Phys. Today*, **48**, 58 (1995).

[7] T.A. Rabedeau, M.F. Torey, R.F. Marks, S.S.P. Parkin, R.F.C. Farrow, and G.R. Harp, *Phys. Rev. B*, **48**, 16810 (1993).

[8] G. Xiao and J.Q. Wang, *J.Appl. Phys.* **75**, 6604 (1994).

[9] R. Krishnan, H. Lassri, M. Seddat and M. Tessier, *J. Appl. Phys.* **75**, 6607 (1994).

[10] M.B. Stearns and Y. Cheng, *J. Appl. Phys.* **75**, 6894 (1994).

[11] J.Q. Wang and G. Xiao, *Phys. Rev. B* **49**, 3982 (1994)

[12] M. Rubinstein, B.N. Das, N.C. Koon, D.B. Chrisey and J. Horwitz, *Phys. Rev. B* **50**, 184 (1994).

[13] P. Allia, M. Knobel, P. Tiberto, and F. Vinai, *Phys. Rev. B* **52**, 15398 (1995).

[14] H. Sang, N. Xu, J.H. Du, G. Ni, S.Y. Zhang and Y.W. Du, *Phys. Rev. B* **53**, 15023 (1996).

[15] M. Kuźmiński, A. Ślawska-waniewska, H.K. Lachowicz, and M. Knobel, *J. Magn. Magn. Mater.* **205**, 7 (1999)

[16] Y.G. Pogorelov, G.N. Kakazei, J.B. Souza, A.F. Kravets, N.A. Lesnik, M.M. Pereira de Azevedo, M. Malinowska and P. Panissod, *Phys. Rev. B* **60**, 12201 (1999).

[17] V.S. Bai, S.M. Bhagat, R. Krishnan, and M. Seddat, *J. Magn. Magn. Mater.* **147**, 97 (1995).

[18] G.N. Kakazei, A.F. Kravets, N.A. Lesnik, M.M. Pereira de Azevedo, Y.G. Pogorelov, and J.B. Souza, *J. Appl. Phys.* **85**, 5654 (1999).

[19] D. Schmool, A. García-Arribas, E. Abad, J.S. Garitaonandia, M.L. Fdez-Gubieda, and J.M. Barandiarán, *J. Magn. Magn. Mater.* **203**, 73 (1999).

[20] H.K. Lachowicz, A. Sienkiewicz, P. Gierlowski and A.S. Waniewska, *J. Appl. Phys.* **88**, 368 (2000).

[21] C. Larica and A.P. Guimarães, *Phys. Stat. Sol. (b)* **77**, k11 (1976).

[22] J. Dubowik, *Phys. Rev. B* **54**, 1088 (1996).

[23] J. Smit and H.C. Beljers, *Philips Res. Rep.* **10**, 113 (1955).

[24] C. Kittel, *Phys. Rev.* **73**, 155 (1948).

[25] D.S. Rodbell, in Magnetism and Metallurgy, Academic, New York, 1969, p. 815.

[26] G.N. Kakazei, A.F. Kravetz, N.A. Lesnik, M.M. Pereira de Azevedo, Yu.G. Pogorelov, G.V. Bondarkova, V.I. Silantiev, J.B. Sousa, *J. Mag. Mag. Mat.* **196-197**, 29 (1999).

[27] E.H.C.P. Sinnecker, I.S. Oliveira, P. Tiberto and A.P. Guimarães, *J. Mag. Mag. Mat.*, (2001), to be published.

[28] J. Wecker, R. von Helmolt, L. Schultz, and K. Samwer, *IEEE Trans. Magn.*, 29 (1993) 3087.

[29] C. Chappert, K. Le Dang, P. Beauvillain, H. Hurdequint and D. Renard, *Phys. Rev.* **34B**, 3192 (1986).